

Pseudospin-filter tunneling of massless Dirac fermions

Zhengdong Li(李政栋) and Wen Zeng(曾文)

Citation: Chin. Phys. B, 2024, 33 (**11**): 117401. DOI: 10.1088/1674-1056/ad78d9
Journal homepage: http://cpb.iphy.ac.cn; http://iopscience.iop.org/cpb

What follows is a list of articles you may be interested in

Anomalous spin Josephson effect in spin superconductors

Wen Zeng(曾文) and Rui Shen(沈瑞)
Chin. Phys. B, 2024, 33 (**3**): 037401. DOI: 10.1088/1674-1056/ad1982

Ac Josephson effect in Corbino-geometry Josephson junctions constructed on Bi_2Te_3 surface

Yunxiao Zhang(张云潇), Zhaozheng Lyu(吕昭征), Xiang Wang(王翔), Enna Zhuo(卓恩娜), Xiaopei Sun(孙晓培), Bing Li(李冰), Jie Shen(沈洁), Guangtong Liu(刘广同), Fanming Qu(屈凡明), and Li Lü(吕力)
Chin. Phys. B, 2022, 31 (**10**): 107402. DOI: 10.1088/1674-1056/ac89d4

Asymmetric Fraunhofer pattern in Josephson junctions from heterodimensional superlattice V_5S_8

Juewen Fan(范珏雯), Bingyan Jiang(江丙炎), Jiaji Zhao(赵嘉佶), Ran Bi(毕然), Jiadong Zhou(周家东), Zheng Liu(刘政), Guang Yang(杨光), Jie Shen(沈洁), Fanming Qu(屈凡明), Li Lu(吕力), Ning Kang(康宁), and Xiaosong Wu(吴孝松)
Chin. Phys. B, 2022, 31 (**5**): 057402. DOI: 10.1088/1674-1056/ac5d30

Cross correlation mediated by distant Majorana zero modes with no overlap

Lupei Qin(秦陆培), Wei Feng(冯伟), and Xin-Qi Li(李新奇)
Chin. Phys. B, 2022, 31 (**1**): 017402. DOI: 10.1088/1674-1056/ac1572

Josephson current in an irradiated Weyl semimetal junction

Han Wang(王含) and Rui Shen(沈瑞)
Chin. Phys. B, 2021, 30 (**7**): 077406. DOI: 10.1088/1674-1056/ac0348

Pseudospin-filter tunneling of massless Dirac fermions

Zhengdong Li(李政栋) and Wen Zeng(曾文)†

Department of Physics, Jiangsu University, Zhenjiang 212013, *China*

(Received 9 July 2024; revised manuscript received 17 August 2024; accepted manuscript online 10 September 2024)

The tunneling of the massless Dirac fermions through a vector potential barrier are theoretically investigated, where the vector potential can be introduced by very high and very thin (δ-function) magnetic potential barriers. We show that, distinct from the previously studied electric barrier tunneling, the vector potential barriers are more transparent for pseudospin-1/2 Dirac fermions but more obstructive for pseudospin-1 Dirac fermions. By tuning the height of the vector potential barrier, the pseudospin-1/2 Dirac fermions remain transmitted, whereas the transmission of the pseudospin-1 Dirac fermions is forbidden, leading to a pseudospin filtering effect for massless Dirac fermions.

Keywords: tunneling junction, pseudospin filter, magnetic barrier

PACS: 74.50.+r, 73.43.jn **DOI:** 10.1088/1674-1056/ad78d9

1. Introduction

The pseudospin-1/2 massless Dirac fermions have been widely investigated since the graphene-like materials[1–4] were successfully fabricated in experiments. Novel phenomena have been found in pseudospin-1/2 massless Dirac system, such as the quantum spin Hall effect,[5–7] specular Andreev reflection,[8] Fabry–Pérot interference,[9–11] Klein tunneling,[12] and laser irradiation-induced pseudospin filter.[13] Furthermore, the pseudospin-1 Dirac system featured by the flat band cutting through the Dirac point can also be realized in condensed matter system, such as the photonic crystals,[14,15] Lieb,[16] and α–$\mathcal{T}_3$[17] lattices. The dispersionless flat band leads to various unique phenomena, such as the super-Klein tunneling,[17–24] super-Andreev reflection,[25,26] and Seebeck and Nernst effects.[27]

The electron tunneling through the electrostatic potential has been widely reported in the literature. It is shown that the electrons with different pseudospins exhibit different behaviors through the electrostatic potential tunneling process.[28–31] The Klein tunneling with the perfect transmission probability occurs only at the normal incidence for the pseudospin-1/2 Dirac fermions, whereas this perfect tunneling can be extended to omnidirection in pseudospin-1 Dirac systems, which is termed as the super-Klein tunneling.[22–24] Consequently, the electrostatic potential barriers are more transparent for the pseudospin-1 Dirac fermions than the pseudospin-1/2 Dirac fermions.

However, the research on the electron tunneling through the vector potential barriers[32–37] is insufficient. Motivated by this fact, here we theoretically study the electron tunneling through the vector potential barrier introduced by the very high and very thin (δ-function) magnetic potential barriers. Both the pseudospin-1/2 and pseudospin-1 Dirac fermions are considered. We find that the transmission probabilities become zero for the pseudospin-1 Dirac fermions but nonzero for the pseudospin-1/2 Dirac fermions with the increasing of the magnetic potential, resulting in a pseudospin filtering effect for massless Dirac fermions.

The paper is organized as follows. The model is presented in Section 2. The results and discussion are shown in Section 3. Finally, we conclude in Section 4.

2. Model

We consider the tunneling junction in the x–y plane with the potential barrier in the region $0 < x < L$, as shown in Fig. 1. The out-of-plane magnetic potential is given by $\boldsymbol{B} = (0, 0, B_z)$ with

$$B_z = \ell_B B_0(\delta(x) - \delta(x-L)), \tag{1}$$

where $\ell_B = \sqrt{c/eB_0}$ is the magnetic length and L is the width of the barrier region. The δ-type magnetic potential barriers are located at the left and right end of the strip, with their magnitudes being B_0 and $-B_0$, respectively. The vector potential induced by $\boldsymbol{B} = \nabla \times \boldsymbol{A}$ reads $\boldsymbol{A} = (0, A_y, 0)$, where

$$A_y = \ell_B B_0(\Theta(x) - \Theta(x-L)). \tag{2}$$

In experiments, the vector potential in our model can be induced by depositing ferromagnetic strips on the top of junction layer but in a way that there is no electrical contact between the junction and these strips.[37,38] The typical experimental value for the magnetic field is $B_0 = 4$ T,[34] where the magnetic length and the vector potential are $\ell_B = 13$ nm and $A_y = 52$ T·nm, respectively.

The tunneling process is described by the low-energy Hamiltonian

$$\mathcal{H} = v_{\mathrm{F}}\left(\boldsymbol{p} + \frac{e}{c}\boldsymbol{A}\right) \cdot \boldsymbol{\Sigma} + V(x), \tag{3}$$

†Corresponding author. E-mail: zeng@ujs.edu.cn

© 2024 Chinese Physical Society and IOP Publishing Ltd

where $\boldsymbol{p}=\hbar\boldsymbol{k}$ is the momentum with $\boldsymbol{k}$ being the wave vector, $V(x)$ is zero for the pristine regions (region I and region III in Fig. 1(a)) and $V(x)=V_0$ for the barrier region (region II in Fig. 1(a)), which can be adjusted by doping or by a gate voltage, and $\boldsymbol{\Sigma}$ is the Pauli matrix. For pseudospin-1/2 fermions, $\boldsymbol{\Sigma}=(\sigma_x,\sigma_y)$,[12,39,40] where

$$\sigma_x=\begin{pmatrix}0&1\\1&0\end{pmatrix},\quad \sigma_y=\begin{pmatrix}0&-\mathrm{i}\\\mathrm{i}&0\end{pmatrix}. \tag{4}$$

For pseudospin-1 fermions, $\boldsymbol{\Sigma}=(S_x,S_y)$,[19,25] where

$$S_x=\frac{1}{\sqrt{2}}\begin{pmatrix}0&1&0\\1&0&1\\0&1&0\end{pmatrix},\quad S_y=\frac{1}{\sqrt{2}}\begin{pmatrix}0&-\mathrm{i}&0\\\mathrm{i}&0&-\mathrm{i}\\0&\mathrm{i}&0\end{pmatrix}. \tag{5}$$

The scattering states can be obtained by the schrödinger equation

$$\mathcal{H}\psi(x)\,\mathrm{e}^{\mathrm{i}k_y y}=E\psi(x)\,\mathrm{e}^{\mathrm{i}k_y y}, \tag{6}$$

where E and k_y are the incident energy and the conserved transverse wave vector, respectively. The energy dispersion is given by

$$E=\hbar v_{\mathrm{F}}\sqrt{k_x^2+\left(k_y+\frac{1}{\ell_B}\right)^2}. \tag{7}$$

The scattering basis states for pseudospin-1/2 are given by

$$\psi_{\mathrm{p}}^{+}=\begin{pmatrix}1\\\mathrm{e}^{\mathrm{i}\theta}\end{pmatrix}\mathrm{e}^{\mathrm{i}k_{\mathrm{p}}x},\quad \psi_{\mathrm{p}}^{-}=\begin{pmatrix}1\\-\mathrm{e}^{-\mathrm{i}\theta}\end{pmatrix}\mathrm{e}^{-\mathrm{i}k_{\mathrm{p}}x}, \tag{8}$$

and the scattering basis states for the pseudospin-1 Dirac fermions are given by

$$\psi_{\mathrm{p}}^{+}=\begin{pmatrix}\mathrm{e}^{-\mathrm{i}\theta}\\\sqrt{2}\\\mathrm{e}^{\mathrm{i}\theta}\end{pmatrix}\mathrm{e}^{\mathrm{i}k_{\mathrm{p}}x},\quad \psi_{\mathrm{p}}^{-}=\begin{pmatrix}-\mathrm{e}^{\mathrm{i}\theta}\\\sqrt{2}\\-\mathrm{e}^{-\mathrm{i}\theta}\end{pmatrix}\mathrm{e}^{-\mathrm{i}k_{\mathrm{p}}x}, \tag{9}$$

where θ is the incident angle satisfing $\sin\theta=\hbar v_{\mathrm{F}}k_y/(E-V_0)$ and $k_{\mathrm{p}}=(E-V_0)\cos\theta/\hbar v_{\mathrm{F}}$ is the longitudinal wave vector with $p=\{\mathrm{I},\mathrm{II},\mathrm{III}\}$ distinguishing different regions of the junction. Consequently, the scattering states can be written as

$$\psi(x)=\begin{cases}\psi_{\mathrm{I}}^{+}+r\psi_{\mathrm{I}}^{-}, & x<0,\\ a\psi_{\mathrm{II}}^{+}+b\psi_{\mathrm{II}}^{-}, & 0<x<L,\\ t\psi_{\mathrm{III}}^{+}, & x>L.\end{cases} \tag{10}$$

The conservation of the current at the boundary requires the continuity of $(\psi_1,\psi_2)^{\mathrm{T}}$ for the pseudospin-1/2 Dirac fermions and $(\psi_1/\sqrt{2}+\psi_3/\sqrt{2},\psi_2)^{\mathrm{T}}$ for the pseudospin-1 Dirac fermions, where ψ_i $(i=1,2,3)$ is the i-th component of the wave function in Eq. (10).[19,41] The transmission and reflection probabilities are given by $T=|t|^2$ and $R=|r|^2$, respectively. One finds that the transmission probability reads

$$T=\frac{1}{\cos^2(k_{\mathrm{p}}L)+Z^2\,\sin^2(k_{\mathrm{p}}L)}, \tag{11}$$

$$Z=\begin{cases}\dfrac{1-\sin\theta\,\sin\theta'}{\cos\theta\,\cos\theta'}, & \text{pseudospin-1/2},\\[2ex] \dfrac{\cos^2\theta'+\cos^2\theta}{2\,\cos\theta\,\cos\theta'}, & \text{pseudospin-1},\end{cases} \tag{12}$$

where the incident angle θ and the refraction angle θ' satisfy $\sin\theta=\hbar v_{\mathrm{F}}k_y/E$ and $\sin\theta'=\hbar v_{\mathrm{F}}(k_y+1/\ell_B)/(E-V_0)$, respectively.

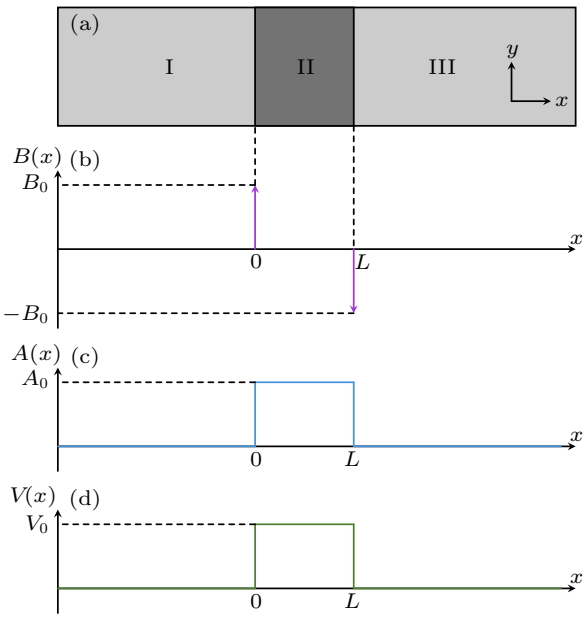


Fig. 1. (a) The schematic illustration of the two-dimensional (2D) tunneling junction in the x–y plane where the transport direction is along the x axis. (b) The profile of the δ-function magnetic potential barriers located at $x=0$ and $x=L$. (c) The vector potential generated by the δ-function magnetic barriers in Fig. 1(b). (d) The electrostatic potential barrier with the magnitude of V_0.

The conductance can be calculated within the Landauer–Büttiker formalism[42–44]

$$G=G_0\int_{-\pi/2}^{\pi/2}\mathrm{d}\theta T\cos\theta, \tag{13}$$

where $G_0=(2e^2/h)N(E)$ is the normalized conductance and $N(E)=(E-V_0)W/\pi\hbar v_{\mathrm{F}}$ with W being the junction width.

3. Results

In the absence of the magnetic field, the incident angle (θ) resolved transmission probability (T) is shown in Fig. 2(a), where the incident energy is $E=0.6V_0$. It is shown that the perfect tunneling with the unit transmission probability for the pseudospin-1/2 Dirac fermions occurs at the normal incidence, i.e., $\theta=0$, as the dashed blue line shown in Fig. 2(a). However, for the pseudospin-1 Dirac fermions, the perfect transmission can be extended to wide incident angles around $\theta=0$, namely, the super-Klein tunneling, as the solid red line shown in Fig. 2(a). It is noted that the angle-resolved scattering pattern is symmetric due to the time-reversal symmetry, i.e., $T(\theta)=T(-\theta)$.

In the presence of the magnetic field, T versus θ is shown in Fig. 2(b). The transverse wave vector is shifted by $k_y \to k_y + 1/\ell_B$. As a result, the scattering pattern is asymmetric since the time-reversal symmetry is broken by the magnetic field, i.e., $T(\theta) \neq T(-\theta)$. The Klein tunneling is absent for both the pseudospin-1/2 and pseudospin-1 Dirac fermions. The maximum value of the transmission probability is about 0.4 for the pseusospin-1/2 Dirac fermions. However, for the pseudospin-1 Dirac fermions, the maximum transmission probability is about 0.05, which is much smaller than that for the pseudospin-1/2 Dirac fermions, indicating that, in contrast to the electrostatic potential barrier, the magnetic field-induced vector potential barrier is more transparent for the pseudospin-1/2 Dirac fernions than the pseudospin-1 Dirac fermions.

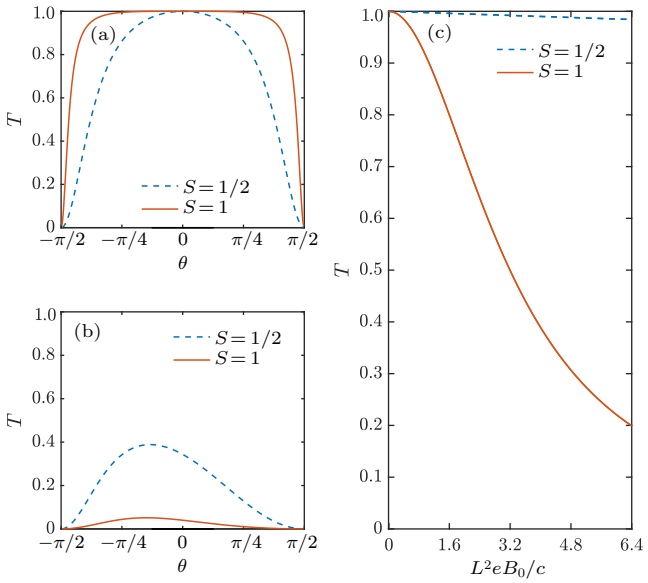


Fig. 2. (a) The transmission probability as a function of the incident angle at $B_0 = 0$ with $E = 0.6V_0$. (b) The transmission probability as a function of the incident angle at $L^2eB_0/c = 2$ with $E = 0.6V_0$. (c) The transmission probability at the normal incidence as a function of B_0 at $k_pL = 0.01$.

The transmission probability at the normal incidence as a function of the magnetic field B_0 is depicted in Fig. 2(c) with $k_pL = 0.01$. It is shown that the transmission probability for the pseudospin-1/2 Dirac fermions ($T_{s=1/2}$) varies smoothly with the increasing of B_0. However, the transmission probability for the pseusospin-1 Dirac fermions ($T_{s=1}$) decreases rapidly with the increasing of B_0. Furthermore, the expressions of the transmission probability at the normal incidence can be obtained analytically as

$$T_{s=1/2} = \frac{1}{\cos^2(k_pL) + \sec^2\theta_B \sin^2(k_pL)}, \tag{14}$$

$$T_{s=1} = \frac{4}{4\cos^2(k_pL) + (\cos\theta_B + \sec\theta_B)^2 \sin^2(k_pL)}, \tag{15}$$

where $\sin\theta_B = 1/\ell_B(E - V_0)$ and $k_p = (E - V_0)\cos\theta_B/\hbar v_F$. For $k_pL \ll 1$, one finds Eq. (14) reads

$$T_{s=1/2} = \frac{1}{(1 + (E - V_0)^2L^2/\hbar^2 v_F^2)},$$

which is independent of B_0. However, the B_0-dependent $T_{s=1}$ is given by

$$T_{s=1} = \frac{4}{(4 + (\cos\theta_B + \sec\theta_B)(E - V_0)^2L^2/\hbar^2 v_F^2))}.$$

For $B_0 \to \infty$, we have $T_{s=1}/T_{s=1/2} \to 0$, as shown in Fig. 2(c).

This pseudospin-filter tunneling can also be explained by the mode matching method as follows. The electron transmission is determined by the boundary condition

$$|\psi_i\rangle + r|\psi_r\rangle = \mathcal{M}_B \cdot t|\psi_t\rangle, \tag{16}$$

where $|\psi_{i(r)}\rangle$ is the incident (reflected) electron state in the left segment of the junction, $|\psi_t\rangle$ is the transmitted electron state in the right segment of the junction, and the magnetic-field-dependent $\mathcal{M}_B$ is the transfer matrix in the middle barrier region. In Eq. (16), r and t are the reflection and transmission amplitudes, respectively. We focus on the electron tunneling at the normal incidence. For both the pseudospin-1/2 and pseudospin-1 Dirac fermions, it is found that $\langle\psi_i|\psi_t\rangle = 0$ at the normal incidence due to the pseudospin-momentum locking. Consequently, the transmission amplitude at the normal incidence can be obtained readily from Eq. (16), namely,

$$t = \langle\psi_i|\mathcal{M}_B|\psi_t\rangle, \tag{17}$$

indicating that the transmission probability ($T = |t|^2$) is directly associated with the transfer matrix $\mathcal{M}_B$, the initial state $|\psi_i\rangle$, and the final state $|\psi_t\rangle$. One finds $\mathcal{M}_B = \cos k_pL + \sin k_pL \sec\theta_B \sin\theta_B\sigma_z - i\sin k_pL \sec\theta_B\sigma_x$ for pseudospin-1/2 Dirac fermions and $\mathcal{M}_B = \cos k_pL - i\sin k_pL\cos\theta_B\sigma_x$ for pseudospin-1 Dirac fermions, where the magnetic angle θ_B satisfies $\sin\theta_B = 1/\ell_B(E - V_0)$ with $\ell_B = \sqrt{c/eB_0}$. With the help of Eq. (17), we have

$$\frac{T_{s=1}}{T_{s=1/2}} \sim \frac{1}{B_0^2}. \tag{18}$$

Consequently, for large B_0, it is found that $T_{s=1} \ll T_{s=1/2}$, indicating that the magnetic barriers are more transparent for pseudospin-1/2 Dirac fermions than for pseudospin-1 Dirac fermions. We note that the super-Klein tunneling can also occur in our magnetic barrier tunneling model, which has the same origin as that predicted in magnetic-field-free tunneling junctions.[24,25,25] In fact, at small incident angles, the tunneling probability can be approximately obtained as $T(\theta) \sim 1 - \theta^4$ for pseudospin-1 Dirac fermions. However, for pseudospin-1/2 Dirac fermions, the deviation was found to be of the order of θ^2.[46] As a result, the nearly perfect transmission can occur in a larger range of the incident angle around $\theta = 0$ for pseudospin-1 Dirac fermions compared with that for pseudospin-1/2 Dirac fermions, namely, the super-Klein tunneling.

The conductance as the function of the incident energy is shown in Figs. 3(a) and 3(b), where the magnetic field is zero in Fig. 3(a) but nonzero in Fig. 3(b). It is shown that in the presence of magnetic field, the conductance of the pseudospin-1/2 Dirac system is much greater than that of the pseudospin-1 Dirac system in the large range of the incident energy, which indicates that the vector potential barrier is more transparent for the pseudospin-1/2 Dirac fermions than the pseudospin-1 Dirac fermions. The conductance as a function of the magnetic field B_0 is shown in Fig. 3(c), where G becomes zero for the pseudospin-1 Dirac system but nonzero for the pseudospin-1/2 Dirac system for large B_0.

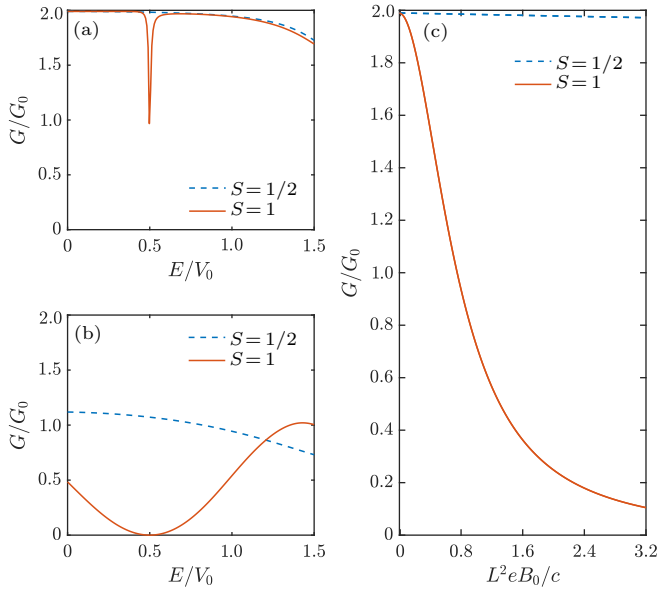


Fig. 3. (a) The conductance as a function of the incident energy at $B_0 = 0$. (b) The conductance as a function of the incident energy at $L^2eB_0/c = 2$. (c) The conductance as a function of B_0 at $k_pL = 0.01$.

4. Conclusion

To conclude, we theoretically investigated the effect of the δ-function magnetic potential barrier on the tunneling effect of Dirac fermions with different pseudospins under electrostatic potential. The pseudospin-1 Dirac fermions exhibits sensitivity to the magnetic potential, while the barrier appears more transparent for the pseudospin-1/2 Dirac fermions. By calculating and comparing the transmission probabilities and conductance of Dirac systems with different pseudospins, we verified the feasibility of utilizing magnetic potential to implement pseudospin filter.

Acknowledgements

Project supported by the College Student Innovation Project (Grant No. 202310299517X) and the Scientific Research Project of Jiangsu University (Grant No. 22A716).

References

[1] Wu Z H, Zhai F, Peeters F M, Xu H Q and Chang K 2011 *Phys. Rev. Lett.* **106** 176802
[2] Jiao M Q and Li Y X 2024 *Phys. Lett. A* **497** 129343
[3] Xu Y F, Fang Y and Jin G J 2023 *New J. Phys.* **25** 013020
[4] Zhao J J, Liu G B, Chen P, Yao Y G, Zhang G Y and Du L J 2024 *Chin. Phys. Lett.* **41** 066801
[5] Kane C L and Mele E J 2005 *Phys. Rev. Lett.* **95** 226801
[6] Beeler M C, Williams R A, Jiménez-García K, LeBlanc L J, Perry A R and Spielman I B 2013 *Nature* **498** 201
[7] Wang J J, Liu S, Wang J and Liu J F 2020 *Phys. Rev. B* **102** 235414
[8] Beenakker C W J 2006 *Phys. Rev. Lett.* **97** 067007
[9] Li Y Q, Chen X R, Luo W, Zhou T and Chen W 2022 *Europhys. Lett.* **137** 36003
[10] Varlet A, Liu M H, Krueckl V, Bischoff D, Simonet P, Watanabe K, Taniguchi T, Richter K, Ensslin K and Ihn T 2014 *Phys. Rev. Lett.* **113** 116601
[11] Mukherjee1 D K, Rao1 S and Das S 2019 *J. Phys.: Condens. Matter* **31** 045302
[12] Wang J J and Wang J 2024 *Chin. Phys. B* **33** 017801
[13] Martinez J C, Jalil M B A and Tan S G 2009 *Appl. Phys. Lett.* **95** 102108
[14] Fang A, Zhang Z Q, Louie S G and Chan C T 2016 *Phys. Rev. B* **93** 035422
[15] Shen R, Shao L B, Wang B G and Xing D Y 2010 *Phys. Rev. B* **81** 041410
[16] Xu Y F and Jin G J 2014 *Phys. Lett. A* **378** 3554
[17] Raoux A, Morigi M, Fuchs J N, Piéchon F and Montambaux G 2014 *Phys. Rev. Lett.* **112** 026402
[18] Singh A and Sharma G 2023 *Phys. Rev. B* **107** 245150
[19] Illes E and Nicol E J 2017 *Phys. Rev. B* **95** 235432
[20] Cunha S M, da Costa D R, Milton Pereira J Jr, Costa Filho R N, Van Duppen B and Peeters F M 2021 *Phys. Rev. B* **104** 115409
[21] Cunha S M, da Costa D R, Milton Pereira J Jr, Costa Filho R N, Van Duppen B and Peeters F M 2022 *Phys. Rev. B* **105** 165402
[22] Korol A M, Sokolenko A I and Shevchenko O 2021 *Low Temp. Phys.* **47** 300
[23] Sukhachov P O, Oriekhov D O and Gorbar E V 2023 *Phys. Rev. B* **108** 075166
[24] Betancur-Ocampo Y, Cordourier-Maruri G, Gupta V and de Coss R 2017 *Phys. Rev. B* **96** 024304
[25] Zeng W and Shen R 2022 *New J. Phys.* **24** 043021
[26] Feng X L, Liu Y, Yu Z M, Ma Z S, Ang L K, Ang Y S and Yang S Y A 2020 *Phys. Rev. B* **101** 235417
[27] Duan W Y 2023 *Phys. Rev. B* **108** 155428
[28] Yang C H, Wieser R and Wang L 2020 *J. Appl. Phys.* **128** 094301
[29] Wang L G and Zhu S Y 2010 *Phys. Rev. B* **81** 205444
[30] Fang A, Zhang Z Q, Louie S G and Chan C T 2019 *Research* **2019** 3054062
[31] Fan C Z, Wang J Q, He J N, Ding P and Liang E J 2013 *Chin. Phys. B* **22** 074211
[32] Lin X, Wang H L, Pan H and Xu H Z 2011 *Chin. Phys. B* **20** 047302
[33] Deng W Y, Zhu R, Xiao Y C and Deng W J 2014 *Chin. Phys. B* **23** 017202
[34] Martino A D, Dell'Anna L and Egger R 2007 *Phys. Rev. Lett.* **98** 066802
[35] Hu X W and Cheng F 2019 *Sci. Rep.* **9** 10947
[36] Yesilyurt C, Tan S G, Liang G and Jalil M B A 2016 *Sci. Rep.* **6** 38862
[37] Mandal I and Sen A 2021 *Phys. Lett. A* **399** 127293
[38] Masir M R, Vasilopoulos P and Peeters F M 2009 *New J. Phys.* **11** 095009
[39] Zalipaev V, Linton C M, Croitoru M D and Vagov A 2015 *Phys. Rev. B* **91** 085405
[40] Allain P E and Fuchs J N 2011 *Eur. Phys. J. B* **83** 301
[41] Zhu R 2024 *Physica B* **687** 416091
[42] Datta S 1992 *Phys. Rev. B* **45** 1347
[43] Cornean H D, Jensen A and Moldoveanu V 2005 *J. Math. Phys.* **46** 042106
[44] Pastawski H M 1991 *Phys. Rev. B* **44** 6329
[45] Contreras-Astorga A, Correa F and Jakubský V 2020 *Phys. Rev. B* **102** 115429
[46] Katsnelson M I, Novoselov K S and Geim A K 2006 *Nat. Phys.* **2** 620